Lanthanide(III) Complexes of 2-[4,7,10-Tris(phosphonomethyl)-1,4,7,10-tetraazacyclododecan-1-yl]acetic Acid (H_7DOA3P): Multinuclear-NMR and Kinetic Studies

by **Maria Paula Campello**[a]), **Marina Balbina**[a]), **Isabel Santos***[a]), **Přemysl Lubal***[b]), **Radek Ševčík**[b]), and **Romana Ševčíková**[b])

[a]) Unidade de Ciências Químicas e Radiofarmacêuticas, Instituto Tecnológico e Nuclear, Estrada Nacional 10, PT-2686-953 Sacavém (phone: +351-219946201; fax: +351-219946185; e-mail: isantos@itn.pt)

[b]) Department of Chemistry, Faculty of Science, Masaryk University, Kotlářská 2, CZ-61137 Brno (phone: +420-549495637; fax: +420-549492494; e-mail: lubal@sci.muni.cz)

Dedicated to Professor *Jean-Claude Bünzli* on the occasion of his 65th birthday in friendship

The protonation constants of 2-[4,7,10-tris(phosphonomethyl)-1,4,7,10-tetraazacyclododecan-1-yl]-acetic acid (H_7DOA3P) and of the complexes $[Ln(DOA3P)]^{4-}$ (Ln = Ce, Pr, Sm, Eu, and Yb) have been determined by multinuclear NMR spectroscopy in the range pD 2–13.8, without control of ionic strength. Seven out of eleven protonation steps were detected (pK_i^H = 13.66, 12.11, 7.19, 6.15, 5.77, 2.99, and 1.99), and the values found compare well with the ones recently determined by potentiometry for H_7DOA3P, and for other related ligands. The overall basicity of H_7DOA3P is higher than that of H_4DOTA and *trans*-H_6DO2A2P but lower than that of H_8DOTP. Based on multinuclear-NMR spectroscopy, the protonation sequence for H_7DOA3P was also tentatively assigned. Three protonation constants (pK_{MHL}, pK_{MH2L}, and pK_{MH3L}) were determined for the lanthanide complexes, and the values found are relatively high, although lower than the protonation constants of the related ligand (pK_3^H, pK_4^H, and pK_5^H), indicating that the coordinated phosphonate groups in these complexes are protonated. The acid-assisted dissociation of $[Ln(DOA3P)]^{4-}$ (Ln = Ce, Eu), in the region c_{H+} = 0.05–3.00 mol dm^{-3} and at different temperatures (25–60°), indicated that they have slightly the same kinetic inertness, being the $[Eu(H_2O)_9]^{3+}$ aqua ion the final product for europium. The rates of complex formation for $[Ln(DOA3P)]^{4-}$ (Ln = Ce, Eu) were studied by UV/VIS spectroscopy in the pH range 5.6–6.8. The reaction intermediate [Eu(DOA3P)]* as 'out-of-cage' complex contains four H_2O molecules, while the final product, $[Eu(DOA3P)]^{4-}$, does not contain any H_2O molecule, as proved by steady-state/time-resolved luminescence spectroscopy.

Introduction. – Acyclic and macrocyclic polyamino chelators bearing coordinating pendant arms have been largely investigated as ligands for lanthanide(III) (Ln^{III}) complexation, looking for compounds suitable for medical applications [1][2]. For such applications, an ideal ligand is the one which forms lanthanide (Ln) complexes with high termodynamic stability and, even more imperative, with extremely high kinetic inertness. Indeed, a high thermodynamic stability does not necessarily prevent complex dissociation *in vivo*, even if a good selectivity for the lanthanide ion over other endogeneous metal ions (*e.g.* Ca^{II}, Zn^{II}, or Cu^{II}) is observed. From solution and biological data, it is also known that the complexes formed with macrocycles are kinetically more inert than analogous complexes with acyclic chelators. Although both

DOTA (= 1,4,7,10-tetraazacyclododecane-1,4,7,10-tetraacetic acid) and DTPA (= *N*,*N*-bis{2-[bis(carboxymethyl)amino]ethyl}glycine) complexes of Gd^{III} have been used as MRI (magnetic resonance imaging) agents, it has been shown that DTPA complexes dissociate under physiological conditions, releasing the metal [3–5]. In nuclear medicine, ^{153}Sm-EDTMP (= ethane-1,2-diylbis(nitrilodimethanediyl)tetrakis(phosphonic acid)) is the only radiolanthanide complex in clinical use. However, due to the acyclic nature of EDTMP, the complex is not kinetically inert, and a large excess of ligand is required to avoid dissociation [6–8].

A great variety of tailor-made ligands designed for the stabilization of lanthanides, aiming at biomedical applications, has been studied and recently reviewed [9][10]. It was shown that the behavior of Ln complexes with potential as radiotherapeutic or MRI agents depends on the Ln ion, backbone of the chelators, nature, and number of the pendant arms [9–15]. In the case of bone targeting, it is clear that bone uptake increases, when the number of phosphonate pendant arms of the macrocycle increases ($[Ln(DOTP)]^{5-} > [Ln(DOA3P)]^{4-} > [Ln(\textit{trans}\text{-DO2A2P})]^{3-}$; Ln = ^{153}Sm, ^{166}Ho) [16–18].

Following our previous work on macrocycle Ln complexes containing phosphonate groups as coordinating pendant arms, we report herein the acid/base behavior of H_7DOA3P and the determination of the protonation constants of several $[Ln(DOA3P)]^{4-}$ complexes (Ln = Ce, Pr, Sm, Eu, and Yb), based on multinuclear NMR spectroscopy. The kinetic properties of some of the Ln^{III} complexes with the title ligand are also presented and discussed.

2. Results and Discussion. – The title ligand (H_7DOA3P) was prepared in a hydrochloride form, according to our method described in [17][18]. For solution studies, the removal of HCl excess and further purification of the ligand was performed on ion-exchange columns. The zwitterionic form of H_7DOA3P was eluted with H_2O, and its composition was confirmed by elemental analysis and ESI-MS (see *Exper. Part*).

2.1. *Acid–Base Behavior of H_7DOA3P.* The acid/base behavior of H_7DOA3P has been studied by multinuclear NMR spectroscopy (^{1}H, ^{13}C, and ^{31}P) in the pD range 2.02–13.80 ($1.62 < pH < 13.40$), without control of the ionic strength. The pattern of the spectra as a function of pD was followed for all nuclei. *Fig. 1* shows the ^{31}P-NMR spectra of H_7DOA3P at different pD values. As can be seen, at pD 2.02 two broad resonances were observed for the P-nuclei a and b (*Fig. 1,a*), while at pD 3.10 only one broad signal was observed, reflecting the presence of a dynamic equilibrium among the protonated and non-protonated species (*Fig. 1,b*). However, the H-atom exchange rate of the phosphonate groups is slow on the NMR timescale, justifying the broadness of the signal. By raising the pD to 4.57, the rate of conversion between protonated and non-protonated species decreases and two, still relatively broad, resonances appear for the P-nuclei (*Fig. 1,c*). These two signals are shifted in opposite directions and converge into a single broad peak at pD 6.31 (*Fig. 1,d*). Above this pD, two resonances can be again observed (*Fig. 1,e*), but at very basic conditions they originate a single sharp signal (*Fig. 1,f*) due to a fast equilibrium between the species in solution. These results indicate clearly the importance of intramolecular H-bonds in the stabilization of different conformations, indicating that when such conformations are no more

stabilized by H-bonds an extremely fast equilibrium between them takes place (*Fig. 1,f*) [19][20].

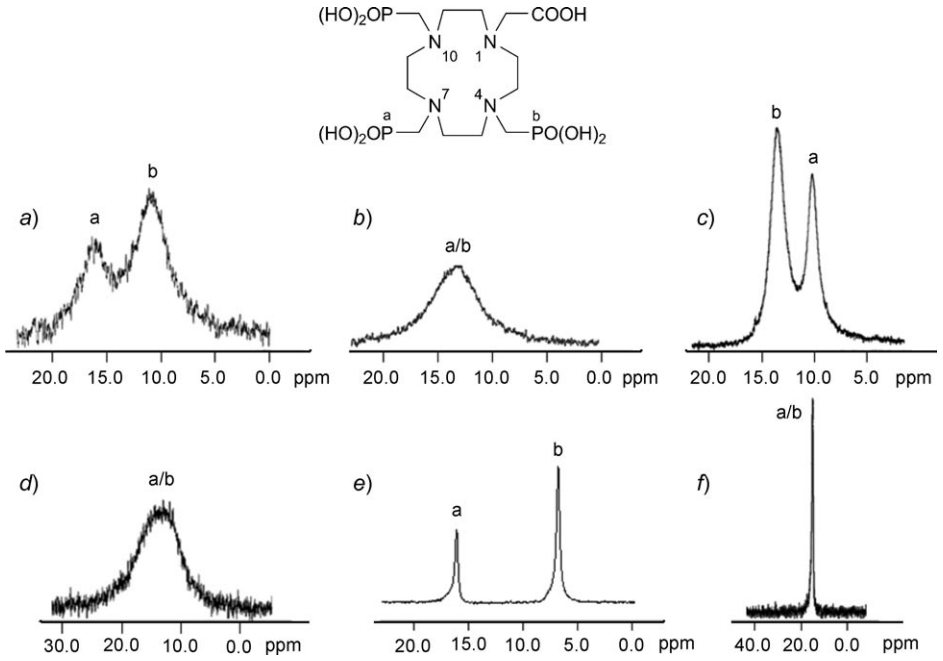

Fig. 1. *^{31}P-NMR Spectra of H_7DOA3P as a function of pD. a*) pD 2.02; *b*) pD 3.10; *c*) pD 4.57; *d*) pD 6.31; *e*) pD 8.16; *f*) pD 13.42.

The protonation constants of H_7DOA3P were determined analyzing the chemical shifts of the CH_2 acetate H-atoms and P-nuclei as a function of pD (*Fig. 2*). The pK_D values were converted to pK_H values, using the correlation $pK_D = 0.11 + 1.10\ pK_H$, determined for polyaza and polyoxa-polyaza macrocyclic compounds [21]. *Table 1* presents the values found for the protonation constants of H_7DOA3P (seven, out of eleven) and, just for comparison, the protonation constants determined by potentiometry for H_7DOA3P [22], and for other related ligands (H_4DOTA, H_5DO3AP, *trans*-H_6DO2A2P, and H_8DOTP) are also shown.

From the data presented in *Table 1*, it can be seen that the protonation constants of H_7DOA3P determined by multinuclear NMR spectroscopy compare well with those determined by *Kálmán*, using potentiometric methods [22]. The overall basicity of H_7DOA3P is higher than that of H_4DOTA and *trans*-H_6DO2A2P, but lower than that of H_8DOTP (*Table 1*), confirming that the overall basicity increases with the number of phosphonate groups [14][15]. Based on the results shown in *Fig. 2*, we have also tentatively assigned a protonation sequence for H_7DOA3P. We have considered that, when a protonation occurs, the H-atoms close to the basic sites are deshielded, this effect being more pronounced when the protonation takes place at the amine adjacent to the CH_2 than at the O-atom of the carboxylate group. It was also considered that the protonation of a given O-atom of a phosphonate group causes a small deshielding of the

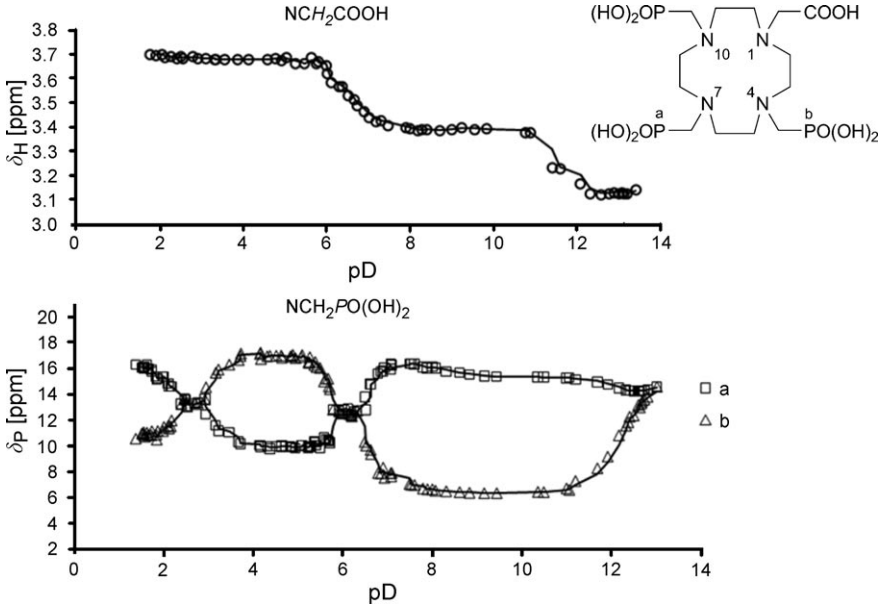

Fig. 2. *^{1}H- and ^{31}P-NMR chemical shifts for H_7DOA3P as a function of pD*

Table 1. *Protonation Constants* (pK_i^H)[a]) *of H_7DOA3P and of Other Related Macrocyclic Ligands.* The standard deviations are given in brackets.

Species[b])	H_7DOA3P[c])	H_7DOA3P[d])	H_4DOTA[e])	H_5DO3AP[f])	*trans*-H_6DO2A2P[g])	H_8DOTP[h])
HL	13.66	13.60(9)	12.74(4)	13.83	13.02	14.65
	13.66(2)					
H_2L	12.11	11.42(2)	9.76(4)	10.35	11.82	12.40
	25.77(2)					
H_3L	7.19	7.69(3)	4.68(4)	6.54	6.35	9.28
	33.07(7)					
H_4L	6.15	6.33(0.3)	4.11(4)	4.34	6.33	8.09
	39.22(1)					
H_5L	5.77	5.13(3)	2.37(5)	3.09	3.13	6.12
	44.9(1)					
H_6L	2.97	2.73(5)		1.63	2.64	5.22
	47.9(1)					
H_7L	1.99	1.62(7)				1.77
	49.9(1)					

[a]) $pK_1 = \log \beta_1$ and $pK_n = \log \beta_n - \log \beta_{n-1}$. [b]) Charges are omitted for clarity. [c]) This work, $T = 21.0°$, determined by ^{31}P-NMR spectroscopy, without control of the ionic strength. The protonation constants ($\log \beta_{hl}$) are in italic ($\beta_n = [H_nL]/([H]^n \times [L])$. [d]) From [22]: $T = 25.0°$, $I = 1.0$M KCl. [e]) From [23]: $T = 25.0°$, $I = 0.1$M Me_4NCl. [f]) From [15]: $T = 25.0°$, $I = 0.1$M Me_4NCl. [g]) From [24]: $T = 25.0°$, $I = 0.1$M Me_4NCl. [h]) From [11]: $T = 25.0°$, $I = 0.1$M Me_4NCl.

P-nuclei, while the protonation of one N-atom causes a pronounced shielding, due to the increase of the electron density around the ^{31}P nuclei [15][19][25][26].

As can be seen in *Fig. 2*, when the pD decreases from 13.8 to 9.1, the P(b)-atoms are shifted strongly upfield and the CH_2 acetate H-atoms are downfield-shifted. These results indicate that the first two protonation constants occur in the $9.1 \leq pD \leq 13.8$ range at the N_4 and N_{10} N-atoms ($\log K_1^H = 13.66$ and $\log K_2^H = 12.11$). Between pD 9.1 and 7.5, no significant changes occur in the ^{31}P and ^{1}H chemical shifts. However, in the pD range 7.5 – 6.2, the $^{31}P(a)$ is upfield-shifted, while $^{31}P(b)$ and the CH_2 H-atoms are strongly downfield-shifted. Such behavior indicates that the two H-atoms attached to N_4 and N_{10} undergo redistribution to N_1 and N_7, while a partial protonation of the phosphonate groups bound to N_4 and N_{10} occurs. In the pD range 6.2 – 4.5, the $^{31}P(b)$ is shifted slightly downfield, certainly due to the protonation/deprotonation of O-atoms of the P(b) groups. In this range, the small change found for the acetate CH_2 H-atoms is probably related to the beginning of the protonation of the O-atoms of the carboxylate group. Decreasing the pD from 4.5 to 2.5 a pronounced change in the ^{31}P resonances and a small change in the CH_2 H-atom resonance indicate that innumerous conformations must occur, due to the redistribution of the NH H-atoms to N_4 and N_{10}, partial protonation/deprotonation of the phosphonate groups, and complete protonation of the carboxylate. Below pD 2.5, only small changes were observed for $\delta(H)$ and $\delta P(b)$, but the $^{31}P(a)$ signal is shifted downfield, most probably due to the protonation of the phosphonate group *trans* to the carboxylate. The protonation of the last two amines and of the remaining O-atoms of the phosphonates could not be detected by NMR, as they certainly occur only under very acidic conditions.

2.2. *Protonation Constants of Ln^{III} Complexes.* The protonation equilibrium for the $[Ln(DOA3P)]^{4-}$complexes (Ln = Ce, Pr, Sm, Eu, and Yb) was investigated by ^{31}P-NMR spectroscopy. In all the pD ranges studied, the complexes present always three distinct resonances, indicating the non-equivalence of the P-nuclei, a quite different pattern from what has been found for $[Ln(DOTP)]^{5-}$ and $[Ln(trans\text{-}DO2A2P)]^{3-}$. The ^{31}P-NMR data found for $[Ln(DOA3P)]^{4-}$ are consistent with a slow exchange between protonated and unprotonated species [24][27]. As an example, the ^{31}P-NMR data for $[Ce(DOA3P)]^{4-}$and $[Yb(DOA3P)]^{4-}$ are shown in *Figs. 3* and *4*.

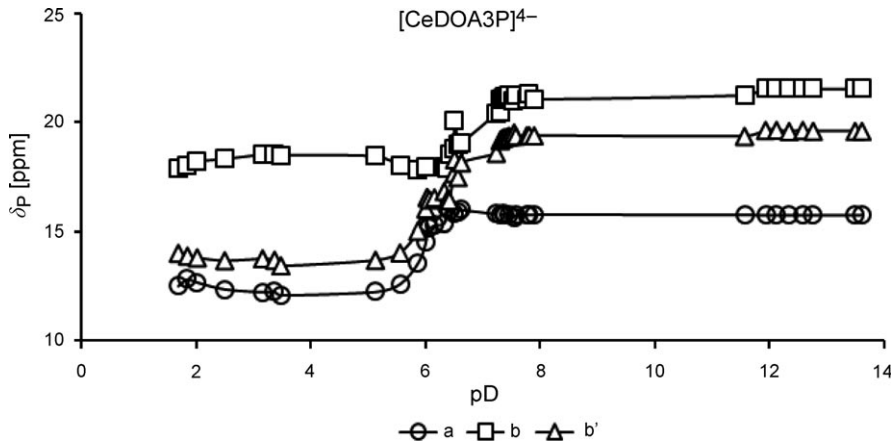

Fig. 3. *^{31}P-NMR Chemical shifts for $[Ce(DOA3P)]^{4-}$ as a function of pD*

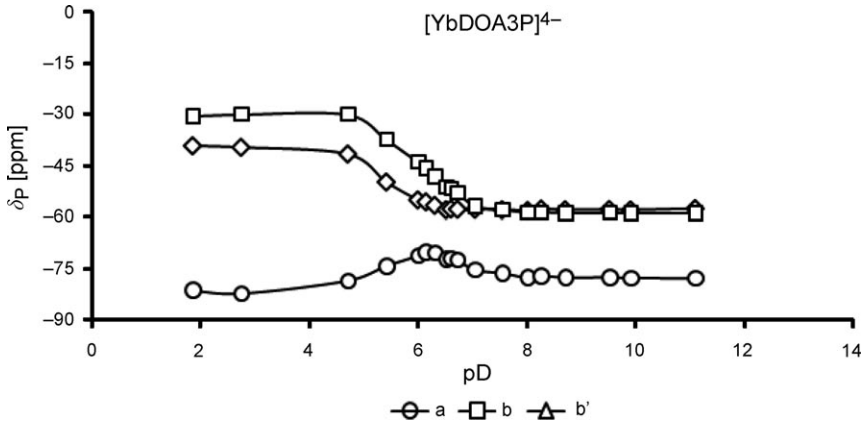

Fig. 4. *^{31}P-NMR Chemical shifts for [Yb(DOA3P)]$^{4-}$ as a function of pD*

All the complexes are stable up to three weeks in slightly acidic conditions (pD > 2; see also the kinetic part of this work, *cf. Table 4* below). The protonation of the three phosphonate groups occurs in the pD range of 8–4. For $[Ce(DOA3P)]^{4-}$, the protonation begins near pD 7.5, as indicated by the shielding of the P-nuclei, but between pD 5.5 and 3.3, a slight change in the direction of one P *cis* to the acetate pendant arm (P(b)) was observed. For $[Yb(DOA3P)]^{4-}$, the protonation starts also near pD 7.5 and is completed near pD 4, but the P-atom *trans* to the acetate pendant arm also changes its direction in the pD range 6–4, a type of inversion which compares well with the behavior found for $[Ln(DOTP)]^{5-}$ (Ln = Eu, Pr, and Nd) [27]. For $[Sm(DOA3P)]^{4-}$ and $[Eu(DOA3P)]^{4-}$, a strong upfield shift is observed for all the P-nuclei, while for $[Pr(DOA3P)]^{4-}$ the P-atoms *cis* and *trans* to the acetate pendant arm are up- and downfield-shifted, respectively. As can be seen in *Table 2*, the protonation constants determined for the Ln complexes do not show any special trend along the lanthanide series, as previously found for $[Ln(DOTP)]^{5-}$, $[Ln(trans\text{-}DO2A2P)]^{3-}$, and $[Ln(DO3AP)]^{2-}$ [15][24][27]. These data indicate that protonations occur on the phosphonate group(s) coordinated to the Ln^{III} ion [15][23][27], being such result supported by the values determined for pK_{MHL}, pK_{MH2L}, and pK_{MH3L} which are lower than those found for pK_3^H, pK_4^H, and pK_5^H [15][28].

2.3. *Kinetic Studies.* From all the $[Ln(DOA3P)]^{4-}$ complexes (Ln = Ce, Pr, Sm, Eu, and Yb) studied by multinuclear NMR spectroscopy, we only performed kinetic studies

Table 2. *Protonation Constants for the [Ln(DOA3P)]$^{4-}$ Complexes Determined by ^{31}P-NMR Spectroscopy* (no control of ionic strength, $T = 21.0°$). The standard deviations are given in brackets.

Ln^{III} ion	pK_{MHL}	pK_{MH2L}	pK_{MH3L}
Ce	6.68(2)	5.80(2)	4.6(1)
Pr	6.92(7)	5.78(7)	4.27(7)
Sm	6.5(2)	5.6(2)	4.1(2)
Eu	6.78(7)	5.80(6)	4.43(6)
Yb	6.89(6)	5.74(6)	4.47(3)

for Ce^{III} and Eu^{III} to compare the results with the ones published in literature [14][15][24][27–33].

2.3.1. *Dissociation of Ln^{III} Complexes.* The dissociation of Ln^{III} complexes can be formulated as

$$-\frac{d[LnL]}{dt} = k_{d,obs}[LnL]_{tot} \quad (1)$$

The empirical rate law for acid-assisted dissociation of Ln^{III} complexes of macrocyclic ligands was determined as usually [14][15]:

$$k_{d,obs} = \frac{k_0 + k \times K \times [H^+]}{1 + K \times [H^+]} = \frac{k_0 + k_H \times [H^+]}{1 + K \times [H^+]} \quad (2)$$

If $K \times [H^+] \gg 1$ (*i.e.*, at low pH), a simpler form can be used

$$k_{d,obs} = k \times K \times [H^+] = k_H \times [H^+] \quad (3)$$

This rate law was based on the assumption that the dissociation mechanism of Ln^{III} complexes of H_7DOA3P [22], *trans*-H_6DO2A2P [24], H_5DO3AP [15], and H_4DOTA [30] is similar and can be described by:

$$[LnL]^{4-} + 3\ H^+ \overset{\beta_{p,3}}{\rightleftharpoons} H_3[LnL]^- \quad (A)$$

$$H_3[LnL]^- + H^+ \overset{K_{p,4}}{\rightleftharpoons} H_4[LnL] \quad (B)$$

$$H_4[LnL] \xrightarrow{k} Ln^{3+} + H_4L^{3-} \quad (C)$$

If the consecutive protonation constants of Ln^{III} complexes, $pK_{MHL} - pK_{MH3L}$, are relatively high (*ca.* 7–4; see *Table 2*), the Ln^{III} complexes are completely transformed (*Reaction A*) to protonated species ($n = 3$ in case of the H_7DOA3P ligand), kinetically inert at pH > 3, since the H-atoms are probably located on the phosphonate groups. The dissociation of the complexes starts with formation of the tetraprotonated species (*Reaction B*) and K_{p4} *ca. K* in *Eqn. 2*). Based on the measurements for the Ce^{III} complex (*Table 3* and *Fig. 5* for $I = 3.0$M and $I = 5.0$M), this species is decomposed (*Reaction C*) in the rate-determining step of the dissociation reaction [14] and it is not charged, supposing no dramatic change of the rate constant on ionic strength.

The completeness of the acid-assisted dissociation for Eu^{III} complex was also studied by luminescence spectroscopy. The reaction was started after addition of perchloric acid ($c(H^+) = 3$ mol dm^{-3}) and the average number of coordinated H_2O molecules to the Eu^{III} was determined as described in [14][29]. The Eu^{III} complex with the title ligand contains probably no H_2O molecule ($\tau = 0.95 - 1.12$ ms for Eu^{III} complex measured in equilibrium at pH 6–7), and the structure of the kinetic intermediate formed must be similar, as indicated by luminescence spectroscopy (*Fig. 6:* number of H_2O molecules is constant during 10 min) and also by the emission spectra (data not shown) with fluorescence intensity of both $^5D_0 \rightarrow {}^7F_1$ and $^5D_0 \rightarrow {}^7F_2$ emission bands

Table 3. *Kinetic Parameters for Acid-Assisted Decomplexation of the [Ln(DOA3P)]$^{3-}$ Complexes* (I = 3.0M (H,Na)ClO_4)

T [°]	k_H [10^{-3} M^{-1} s^{-1}]	K [M^{-1}]	k [10^{-3} s^{-1}]
Ce^{III}			
25.0	0.24 ± 0.01	0.92 ± 0.08	0.3 ± 0.2
40.0	1.5 ± 0.1	1.3 ± 0.1	1.1 ± 0.1
50.0	4.5 ± 0.5	1.6 ± 0.3	2.8 ± 0.6
60.0	11.3 ± 0.4	1.9 ± 0.1	6.0 ± 0.4
60.0[a])	18.8 ± 0.2	3.6 ± 0.5	5.1 ± 0.9
Act./Therm. Parameters	$E_a = 91 \pm 2$ kJ mol^{-1}, $\Delta H^{+} = 89 \pm 2$ kJ mol^{-1}, $\Delta S^{+} = -16 \pm 7$ J K^{-1} mol^{-1}	$\Delta H^0 = 14 \pm 1$ kJ mol^{-1}, $\Delta S^0 = 57 \pm 4$ J K^{-1} mol^{-1}	$E_a = 74.4 \pm 0.9$ kJ mol^{-1}, $\Delta H^{+} = 71.8 \pm 0.9$ kJ mol^{-1}, $\Delta S^{+} = -73 \pm 3$ J K^{-1} mol^{-1}
Eu^{III}			
40.0	2.3 ± 0.9	0.9 ± 0.6	3 ± 1
50.0	11.5 ± 0.8	2.1 ± 0.2	5.4 ± 0.6
60.0	36 ± 3	3.6 ± 0.4	10 ± 1
Act./Therm. parameters	$E_a = 121 \pm 10$ kJ mol^{-1}, $\Delta H^{+} = 118 \pm 10$ kJ mol^{-1}, $\Delta S^{+} = 81 \pm 30$ J K^{-1} mol^{-1}	$\Delta H^0 = 60 \pm 7$ kJ mol^{-1}, $\Delta S^0 = 192 \pm 22$ J K^{-1} mol^{-1}	$E_a = 60 \pm 3$ kJ mol^{-1}, $\Delta H^{+} = 57 \pm 3$ kJ mol^{-1}, $\Delta S^{+} = -111 \pm 8$ J K^{-1} mol^{-1}

[a]) I = 5.0M (H,Na)ClO_4.

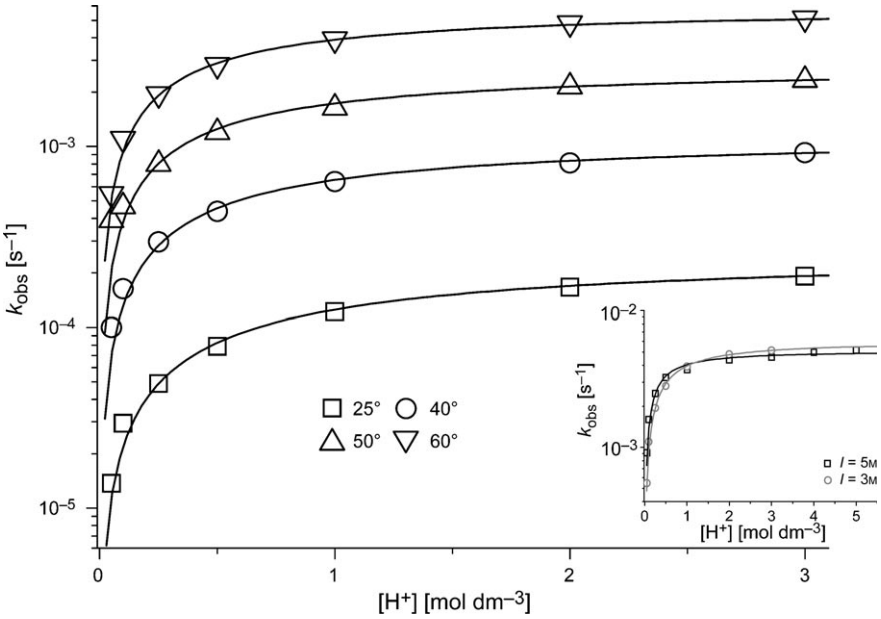

Fig. 5. *The* pseudo-*first-order rate constant dependence on solution acidity for the acid-assisted dissociation of the [Ce(DOA3P)]$^{4-}$ complex* (I = 3.0M (H,Na)ClO_4). In the offset, the comparison of *pseudo*-first-order rate constants for I = 3.0M and I = 5.0M (H,Na)ClO_4 is shown.

simultaneously decreasing. A similar effect was observed for dissociation kinetics of Eu^{III} complexes with the analogous *trans*-H_6DO2A2P and H_8DOTP [24][31]. However, the kinetic inertness of the Eu^{III} complexes is affected by the symmetry of the ligands. As can be seen in *Fig. 6*, the $[Eu(DOTP)]^{5-}$ is not completely decomposed, while the analogous complexes with *trans*-H_6DO2A2P and H_7DOA3P decompose after 1–2 h leading to the $[Eu(H_2O)_9]^{3+}$ ion.

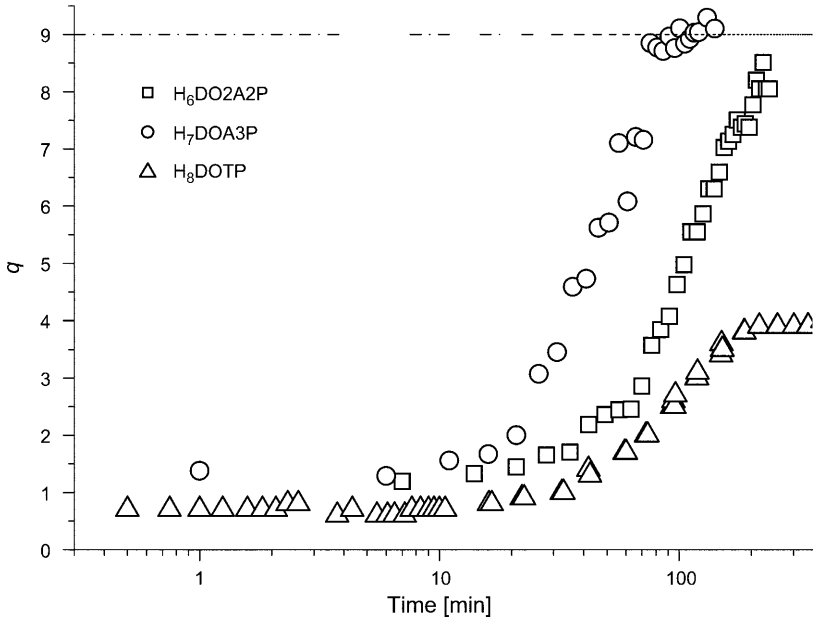

Fig. 6. *The time change of the number of H_2O molecules (q) coordinated to Eu^{III} complex during its acid-assisted dissociation* (c(EuL) *ca.* 0.001–0.010 mol dm^{-3}, $c(HClO_4) = 3.0$ mol dm^{-3}).

The acid-assisted dissociation of the Ce^{III} and Eu^{III} complexes was studied in the region of $c(H^+) = 0.05 - 3.00$ mol dm^{-3}, adjusted by perchloric acid and variable temperature (25–60°). The $[Ce(H_2O)(DOA3P)]^{4-}$ complex, having an absorption maximum at 305 nm, disappears during the dissociation reaction. The wavelength of the absorption maximum can be compared with values found for Ce^{III} complexes with analogous ligands: $[Ce(H_2O)(DOTP)]^{5-}$ (300 nm [32]), $[Ce(H_2O)(DO2A2P)]^{3-}$ (310 nm [24]), $[Ce(H_2O)(DOTA)]^{-}$ (322 nm [33]).

For the $[Ce(H_2O)(DOA3P)]^{4-}$ complex, the dependence of the *pseudo*-first-order rate constant on solution acidity is shown in *Fig. 5*, and the calculated parameters using *Eqn. 2* are given in *Table 3*. The $[Ce(DOA3P)]^{4-}$ complex is slightly of the same kinetic inertness as the $[Eu(DOA3P)]^{4-}$, since they have almost the same tendency to protonation and to decompose.

Using the thermodynamic parameters of the protonation of Ln^{III} complexes, this process is more endothermic for Eu^{III} than for Ce^{III}. On contrary, the activation parameters of dissociation of both Ln^{III} complexes is opposite (see *Table 3*; the associative pathway with rate constant k) contributing more to total kinetic inertness

than the protonation process (see Ce^{III} complex). Both processes are also accompanied by some important structural changes, as it can be seen from the high values of entropic changes (see *Table 3*).

The protonation of Ce^{III} complexes is generally less pronounced than for Eu^{III} [15][23][30] (see *Table 4*). The kinetic inertness of the Ce^{III} and Eu^{III} complexes, when the number of phosphonate functional groups change from zero to four (H_4DOTA – H_8DOTP), can be evaluated according to different parameters (*e.g.*, k_0, k_H, K (parameters of *Eqn. 2*)). Since some parameters of *Eqn. 2* are missing for the Ce^{III} complex, the observed *pseudo*-first-order rate constants at low (pH 2) and high ($[H^+]_{tot} = 3.0$M) acidities seem to be more suitable (see *Fig. 7*). For the Ce^{III} complex, the substitution of smaller acetic acid pendant arms by more bulky phosphonates leads to higher kinetic inertness, while this effect is less pronounced and opposite for the Eu^{III} complex (*Fig. 7*). Decreasing the Ln^{III} ionic radius (Ce^{III} *vs.* Eu^{III}), the kinetic inertness is much higher for Eu^{III} complexes with ligands having a lower number of phosphonic pendant arms (H_4DOTA, H_5DO3AP) than for Ce^{III}. In addition, the difference between both Ln^{III} complexes diminishes for ligands having a higher number of phosphonates (*trans*-H_6DO2A2P, H_7DOA3P, H_8DOTP).

Table 4. *Kinetic Parameters for Acid-Assisted Decomplexation of the Ln^{III} Complexes with DOTA-Like Ligands* ($T = 25°$, $I = 3.0$M (Na,H)ClO_4)

Ligand	k_H [10^{-4} M^{-1} s^{-1}]	K [M^{-1}]	k [10^{-4} s^{-1}]	$k_{d,obs}$ [10^{-6} s^{-1}] (pH 2)	$k_{d,obs}$ [10^{-4} s^{-1}] ($[H^+] = 3.0$M)	Ref.
Ce^{III}						
H_4DOTA	8; 20[a])	–	–	8.2[a])	204[a])	[30]
H_5DO3AP	12.2		–	12	36.6	[15]
H_6DO2A2P	3.5	0.19	18	3.5	6.71	[24]
H_7DOA3P	2.4	0.92	3	2.4	1.91	This work
H_8DOTP	0.46	3.3[b])	–	0.46	1.18	[32]
Eu^{III}						
H_4DOTA[c])	0.14; 10[a])	14; 0.12[a])	0.01; 6.2[a])	0.21	1.6	[30]
H_5DO3AP	0.98	0.21	4.6	0.96	1.8	[14]
H_6DO2A2P	5.2	1.64	3.2	5.1	2.6	[24]
H_7DOA3P	2.35	0.29	8.0	2.3	4.1	This work
H_8DOTP	9.8	2.0	6.2	1.2	5.6	[31]

[a]) $k_{obs} = k_{H1} \times [H^+] + k_{H2} \times [H^+]^2$. [b]) $T = 50°$. [c]) $k_{obs} = \dfrac{k_{d,1} \times K_1 \times [H^+] + k_{d,2} \times K_1 \times K_2 \times [H^+]^2}{1 + {}^{H}K_1 \times [H^+] + {}^{H}K_1 \times {}^{H}K_2 \times [H^+]^2}$.

2.3.2. *Formation of Ln^{III} Complexes.* The kinetics of formation of Ce^{III} and Eu^{III} complexes was studied in slightly acidic medium (pH 5.6–6.8) where the complex formation is complete, and it is still relatively slow in order to be followed by conventional molecular absorption spectroscopy. The rate of complex formation between the Ce^{III} ion and the ligand can be written as second-order rate law

$$v = k_2^f \times [L]_{tot} \times [Ce^{3+}]_{tot} \quad (4)$$

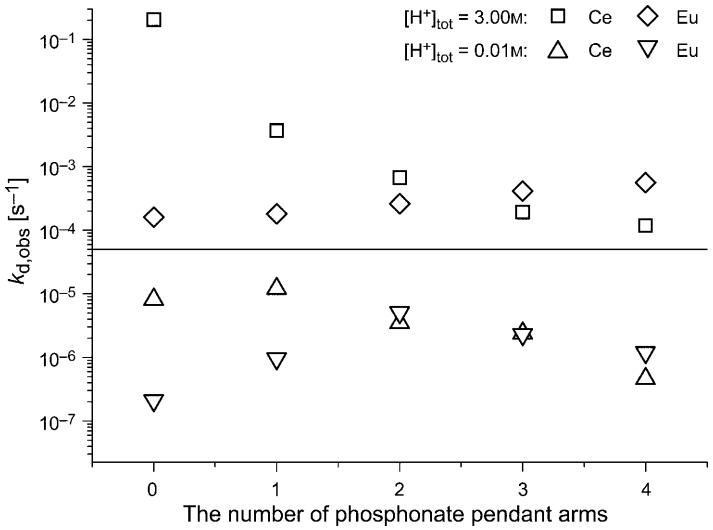

Fig. 7. *The comparison of reactivity of Ln^{III} complexes with DOTA-like macrocyclic ligands having different number of phosphonic pendant arms measured* (DOTA $n_P = 0$, DOTP $n_P = 4$) *at* $T = 25°$

and the second-order rate constants determined for various pH are dependent on the H-atom concentration

$$k_2^f = \frac{\sum_{i=0}^{n} {}^f k_{\mathrm{H}i\mathrm{L}} \times \beta_{\mathrm{p},i} \times [\mathrm{H}^+]^i}{\alpha_{\mathrm{L}}} \tag{5}$$

where the denominator is

$$\alpha_{\mathrm{L}} = \beta_{\mathrm{p},7} \times [\mathrm{H}^+]^7 + \beta_{\mathrm{p},6} \times [\mathrm{H}^+]^6 + \beta_{\mathrm{p},5} \times [\mathrm{H}^+]^5 + \beta_{\mathrm{p},4} \times [\mathrm{H}^+]^4 + \beta_{\mathrm{p},3} \times [\mathrm{H}^+]^3 + \beta_{\mathrm{p},2} \times [\mathrm{H}^+]^2 + \beta_{\mathrm{p},1} \times [\mathrm{H}^+] + 1 \tag{6}$$

using the ligand protonation constants $\beta_{\mathrm{p},n}$ defined as

$$\beta_{\mathrm{p},i} = \frac{[\mathrm{H}_i\mathrm{L}]}{[\mathrm{H}^+]^i[\mathrm{L}]} \tag{7}$$

Assuming the same ionic strength effect (1.0M → 0.1M) as for the analogous ligand *trans*-H_6DO2A2P [24][28], the protonation constants of H_7DOA3P for $I = 0.1$M KCl were recalculated from the values: 13.6; 11.42; 7.69; 6.33; 5.13; 2.73, $I = 1.0$M KCl, $T = 25°$ [22]. The recalculated values (14.22, 11.81; 8.08; 6.51; 5.38; 2.86) have been used in order to fit the rate constants k_2^f as a function of solution acidity (see dashed lines in *Fig. 8*) according to the *Eqn. 5*. The same procedure was applied using the protonation constants obtained in this work (see *Table 1*, fits are full lines in *Fig. 8*). The species

H_3L^{4-} and H_2L^{5-} seem to be active for the reaction with Ln^{III} ions, and the calculated partial rate constants are not so sensitive to the applied set of protonation constants (see *Table 5*). In addition, the difference in reactivity of both protonated species towards Ln^{III} ions is not remarkable, similarly as in the dissociation reaction, due to the similar structure of both active species, in which there is no additional structure stabilization by H-bonds [15]. On contrary to H_4DOTA and H_5DO3AP ligands [14][15][30], both Ce^{III} and Eu^{III} ions are taking place in the complexation reaction by the same rate.

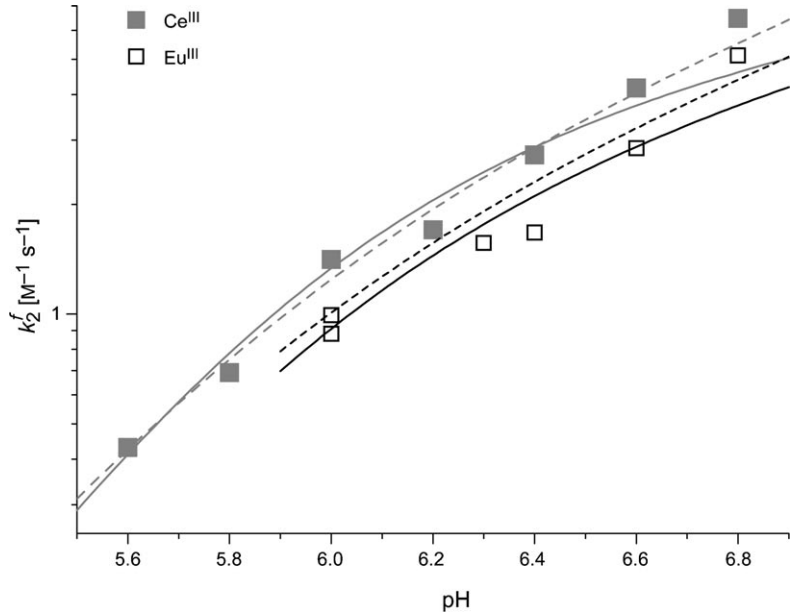

Fig. 8. *Formation of Ln^{III} complexes with H_7DOA3P as a function of pH* ($c(Ce) = 2 \times 10^{-4}$ M, $c(L) = 4 \times 10^{-4}$ M, or $c(Eu) = 5 \times 10^{-4}$ M, $c(L) = 1 \times 10^{-3}$ M, both $I = 0.10$M KCl, $T = 25°$). The experimental points are fitted by function (see *Eqn. 5* in the text) with parameters given in *Table 5*.

Table 5. *The Survey of Kinetic Parameters for Complexation of the $[Ln(DOA3P)]^{3-}$ Complexes* (the charges are omitted for the sake of clarity)

Ln^{III} ion	$k(H_3L)$ [M^{-1} s^{-1}]	$k(H_2L)$ [M^{-1} s^{-1}]	Ratio $k(H_2L)/k(H_3L)$
Ce^{III}	$3.8_2 \pm 0.2_6$[a])	$9._3 \pm 4._9$[a])	2.4[a])
	$5.7_8 \pm 0.2_8$[b])	57 ± 40[b])	9.9[b])
Eu^{III}	$2.4_2 \pm 0.3_7$[a])	$9._2 \pm 3._6$[a])	3.8[a])
	$4.3_9 \pm 0.4_2$[b])	28 ± 33[b])	5.7[b])

[a]) Calculated with protonation constants given in this work for variable ionic strength $I = 0.02 - 0.52$M (see *Table 1*). [b]) Calculated with protonation constants taken from [22], $I = 1.0$M KCl, and corrected for $I = 0.1$M KCl.

To throw light on the reaction mechanism, the time-resolved laser spectroscopy was employed to study Eu^{III} complex formation when the average number of H_2O

molecules was determined in the course of Eu^{III} complex formation (see *Fig. 9*). As it can be seen, the $[Eu(DOA3P)]^{4-}$ complex formation is slower in comparison with analogous ligands (*e.g.*, H_4DOTA, H_5DO3AP) studied at pH *ca.* 5.6 [14], and it is also shifted to higher pH 6.5. The time dependence of H_2O molecules bound in Eu^{III} complex (*Fig. 9*) were fitted (for more details, see [14]) and the following parameters were estimated: $q(EuL^*) = 3.8 \pm 0.5$, $q(EuL) = 1.4 \pm 0.5$, $k_{f,obs} = (1.7_5 \pm 0.3_0) \times 10^{-2}$ $min^{-1} = (2.9_1 \pm 0.5_0) \times 10^{-4}$ s^{-1}. The number of H_2O molecules in the final product was measured after 24 h and it was determined to be *ca.* 0.7 ± 0.5, which is in agreement with the value $(0.2-0.4) \pm 0.5$ determined from the thermodynamic experiment. On the contrary, the value 1.4 ± 0.5 determined in the kinetic experiment is caused by the fact that the reaction was not already finished (see *Fig. 9*). The structure of the EuL* reaction intermediate is $[EuL(H_2O)_4]$, similar to the one proposed earlier for H_5DO3AP [15] and *trans*-$H_6DO2A2P$ ligands [24]. The rate constant determined in this study is comparable to the one found for the analogous system Eu^{III}-$H_6DO2A2P$ at pH 5.5 [24]. The rate-determining step is the transfer of Eu^{III} ion into the macrocyclic cavity when 'out-of-cage' Eu^{III} complex with bound pendant arms is transformed to fully coordinated 'in-cage' complex as final product (see Scheme in [14]).

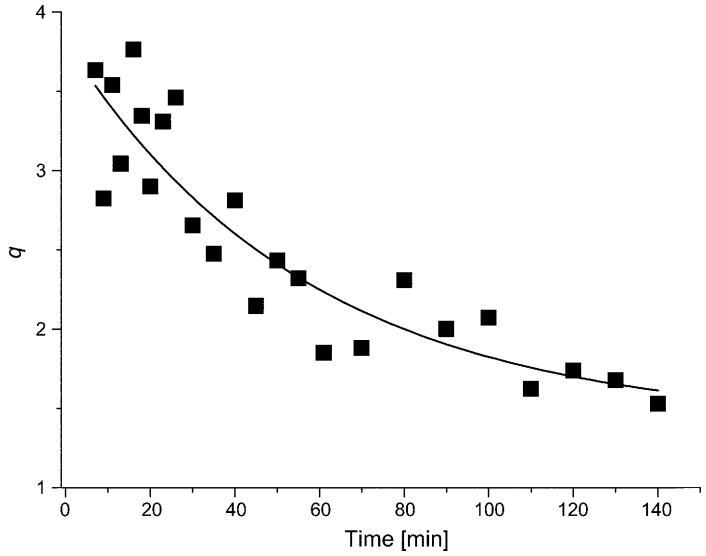

Fig. 9. *Time dependence of change in the number of bound H_2O molecules (q) during formation of the Eu^{III} complex with H_7DOA3P* ($c(Eu) = 5 \times 10^{-4}$ M, $c(L) = 1 \times 10^{-3}$ M, pH 6.5, $I = 0.10$M KCl, $T = 25°$)

Concluding Remarks. – Based on multinuclear NMR studies, seven protonation constants for 2-[4,7,10-tris(phosphonomethyl)-1,4,7,10-tetraazacyclododecan-1-yl]acetic acid (H_7DOA3P) were determined ($pK_i^H = 13.66$, 12.11, 7.19, 6.15, 5.77, 2.99, and 1.99), and a protonation sequence was proposed. As expected, the overall basicity of H_7DOA3P is higher than that of H_4DOTA, H_5DO3AP, and *trans*-$H_6DO2A2P$, but lower than that of H_8DOTP. The protonation constants of the lanthanide complexes $[Ln(DOA3P)]^{4-}$ (Ln = Ce, Pr, Sm, Eu, and Yb) were also determined by multinuclear

NMR spectroscopy, without control of ionic strength. The values found are lower than those of the related free ligand (pK_3^H, pK_4^H, and pK_5^H), indicating the protonation of the phosphonate groups.

The acid-assisted dissociation of $[Ln(DOA3P)]^{4-}$ (Ln = Ce and Eu) and the kinetics of complex formation were studied by UV/VIS spectroscopy and by steady-state/time-resolved luminescence spectroscopy, at different pH and temperatures. The kinetic inertness of the complexes is slightly the same, since they have almost the same tendency to protonation and decomposition. The species $(H_3DOA3P)^{4-}$ and $(H_2DOA3P)^{5-}$ seem to be active for reaction with Ln^{III} ions and the difference in reactivity is not remarkable, due to the similar structure of both active species. The reaction intermediate is $[Eu(DOA3P)(H_2O)_4]$*, and the rate-determining step is the transfer of the Eu^{III} ion into a macrocyclic cavity when an 'out-of-cage' Eu^{III} complex with bound pendant arms is transformed to the fully coordinated 'in-cage' $[Eu(DOA3P)]^{4-}$ complex.

Experimental Part

1. *Reagents.* Chemicals and solvents were of reagent grade and were used without further purification, unless stated otherwise. D_2O, hydrochloric deuterium and $LnCl_3$ (Ln = Ce, Pr, Sm, Eu, and Yb) were obtained from *Aldrich Chemical Co.* and *Alfa Aesar Co.* (Germany), and the aq. stock solns. were standardized by chelatometric titration. KOD was freshly prepared before use. 2-[4,7,10-Tris(phosphonomethyl)-1,4,7,10-tetraazacyclododecan-1-yl]acetic acid (H_7DOA3P) was prepared as previously reported [17][18].

2. *Anal. Methods.* pH Measurements: *ORION SA 720* potentiometer; pH of the solns. were measured with a microelectrode *Mettler-Toledo U402-M3-S7/200*. ^1H- (300 MHz), ^{13}C- (75.5 MHz), and ^{31}P- (121.5 MHz) NMR spectra: *Varian Unit Inova-300* spectrometer at 293 K; in D_2O; ^1H-, ^{13}C-, and ^{31}P-NMR chemical shifts (δ) are given in ppm relative to TMS (internal reference; ^1H, δ 0.0), to 1,4-dioxane (external reference; δ ^1H: 3.75; ^{13}C: 69.20), and to 85% aq. H_3PO_4 soln. (external reference; ^{31}P, δ 0.0), resp. MS: LCQ ion trap mass spectrometer (*Thermo Finnigan*, San Jose, CA, USA) equipped with an electrospray ionization (ESI), operating in negative mode. Elemental analysis: automatic analyser *EA 1100 CE Instruments.*

All kinetic measurements were carried out on a double-beam spectrometer *UV 2* (*Pye Unicam*, UK), a diode array spectrophotometer *HP-8453A* (*Hewlett-Packard*, USA) and/or *Aminco Bowman AB2* fluorimeter (*Aminco Bowman*, USA).

3. *Purification of H_7DOA3P.* The title ligand, H_7DOA3P, was synthesized in a hydrochloride form as previously described [17][18]. The hydrochloride (2.4 g) was dissolved in H_2O and purified first on a *Dowex 50* column (3.5 × 20 cm, H^+ form) by elution with H_2O and followed by 10% aq. pyridine. The pyridine fractions were evaporated to dryness. The concentrated aq. soln. of the residue was absorbed on an *Amberlite CG50* column (3.5 × 20 cm, H^+-form) and the column was eluted with H_2O. Early fractions containing the pure zwitterionic form of the title product were combined, and H_2O was evaporated close to dryness to give a white solid. The white solid was filtered, washed with H_2O, and vacuum-dried yielding $H_7DOA3P \cdot 2\,H_2O$ (2.1 g). Anal. calc. for $C_{13}H_{35}N_4O_{13}P_3$ (548.36): C 28.47, H 6.43, N 10.22; found: C 28.14, H 6.57, N 10.34. ESI-MS (neg.): 511 ($[M-H]^-$).

4. *NMR Experiments.* 4.1. *^1H- and ^{31}P-NMR Titration of H_7DOA3P.* Solns. of H_7DOA3P (*ca.* 2×10^{-3} M) for NMR measurements were prepared in D_2O and the pD value was adjusted by adding DCl or CO_2-free KOD. The solns. were allowed to stabilize and the final pH was determined directly in the NMR-tube with a combination microelectrode *Mettler-Toledo U402-M3-S7/200*, calibrated at $21 \pm 0.5°$ with three standard buffers (pH 4.01, 7.00, and 9.21). The pD measurements were performed without control of the ionic strength. The pD was calculated according to the equation $pD = pH^* + (0.40 \pm 0.02)$ [34], where pH* corresponds to the reading of the pH meter. The protonation constants of H_7DOA3P

were calculated with the HYPNMR program using the δ(H) and δ(P) of the ligand at the different pD values [35].

4.2. *^{31}P-NMR Titration of Ln Complexes.* Ln^{III}-DOA3P solns. for the ^{31}P-NMR pH-titration were prepared as follows: 0.3 ml of a soln. of H_7DOA3P in D_2O (10 mM) was neutralized, with a freshly prepared soln. of KOD (*ca.* 1.5M), and a stoichiometric amount of $LnCl_3$ was added (Ln = Ce, Pr, Sm, Eu, and Yb). After full formation of the complexes (evidenced by stabilization of the pD), each soln. was adjusted to high pD (*ca.* 13) with KOD and then titrated to low pD with DCl, while monitoring the ^{31}P-NMR spectra. The pH of the solns. was determined in the same way as described above for the ligand.

5. *Kinetic Measurements.* The experimental methodology for the kinetic studies on the $[Ln(DOA3P)]^{4-}$ complexes was the same as described in [24][26][28]. All spectroscopic kinetic measurements were carried out on a double-beam spectrometer *UV 2* (*Pye Unicam*, UK), a diode array spectrophotometer *HP-8453A* (*Hewlett-Packard*, USA) and/or *Aminco Bowman AB2* fluorimeter (*Aminco Bowman*, USA). Dissociation kinetics of the Ln^{III} complexes was followed at ionic strength I = 3.0 mol dm^{-3} (H,Na)ClO_4 (c(LnL) *ca.* $(1-2.5)\times10^{-3}$ mol dm^{-3}), and at the H-atom concentration varied in the range of 0.05–3.00 mol dm^{-3}. The decomplexation and complexation reaction of the $[Eu(DOA3P)]^{4-}$ was followed by a change of emission spectra (Eu: λ_{exc} = 394 nm). The absorption spectra at the CT band (Ce: 305 nm) were used to study formation and dissociation kinetics of $[Ce(DOA3P)]^{4-}$. The activation parameters for the Ln^{III} complex dissociation were obtained from the temp. dependence in region 25–60°. Data from kinetic experiments were processed by non-linear regression using EXCEL, HP, and/or PROK-II [36] software with identical results, and the measured values of the analytical signal were corrected for a background signal. The experimental methodology for the TRFLS experiments and their application in kinetic studies were described in [14][31]. The precision for the coordinated H_2O molecules determined was estimated as $\pm$0.5, based on published data [29], and refs. cit. therein.

This study was performed under the frame of the *EU COST D38* program.

REFERENCES

[1] M. Bottrill, L. Kwok, N. J. Long, *Chem. Soc. Rev.* **2006**, *35*, 557.
[2] F. Rösch, E. Forssell-Aronsson, 'Radiolanthanides in Nuclear Medicine', in 'Metal Ions in Biological Systems', Eds. A. Sigel, H. Sigel, Dekker, New York, 2004, Vol. 42, p. 77.
[3] J. M. Idée, M. Port, I. Raynal, M. Schaefer, S. Le Greneur, C. Corot, *Fundam. Clin. Pharmacol.* **2006**, *20*, 563.
[4] L. Sarka, L. Burai, R. Király, L. Zékány, E. Brücher, *J. Inorg. Biochem.* **2002**, *91*, 320.
[5] P. Caravan, J. J. Ellison, T. J. McMurry, R. B. Lauffer, *Chem. Rev.* **1999**, *99*, 2293.
[6] A. N. Serafini, S. J. Houston, I. Resche, D. P. Quick, F. M. Grund, P. J. Ell, A. Bertrand, F. R. Ahmann, E. Orihuela, R. H. Reid, R. A. Lerski, B. D. Collier, J. H. McKillop, G. L. Purnell, A. P. Pecking, F. D. Thomas, K. A. Harrison, *J. Clin. Oncol.* **1998**, *16*, 1574.
[7] W. A. Volkert, J. Simon, A. R. Ketring, R. A. Holmes, L. C. Lattimer, L. A. Corwin, *Drugs Future* **1989**, *14*, 799.
[8] W. A. Volkert, T. J. Hoffman, *Chem. Rev.* **1999**, *99*, 2269.
[9] P. Hermann, J. Kotek, V. Kubíček, I. Lukeš, *Dalton Trans.* **2008**, 3027.
[10] S. Liu, *Adv. Drug. Deliv. Rev.* **2008**, *60*, 1347.
[11] F. Marques, L. Gano, M. P. Campello, S. Lacerda, I. Santos, L. M. P. Lima, J. Costa, P. Antunes, R. Delgado, *J. Inorg. Biochem.* **2006**, *100*, 270.
[12] F. Marques, K. P. Guerra, L. Gano, J. Costa, M. P. Campello, L. M. P. Lima, R. Delgado, I. Santos, *J. Biol. Inorg. Chem.* **2004**, *9*, 859.
[13] F. Marques, L. Gano, M. P. Campello, S. Lacerda, I. Santos, *Radiochim. Acta* **2007**, *95*, 335.
[14] P. Táborský, I. Svobodová, P. Lubal, Z. Hnatejko, S. Lis, P. Hermann, *Polyhedron* **2007**, *26*, 4119.
[15] P. Táborský, P. Lubal, J. Havel, J. Kotek, P. Hermann, I. Lukeš, *Collect. Czech. Chem. Commun* **2005**, *70*, 1909.
[16] M. P. Campello, F. Marques, L. Gano, S. Lacerda, I. Santos, *Radiochim. Acta* **2007**, *95*, 329.

[17] L. Gano, F. Marques, M. P. Campello, M. Balbina, S. Lacerda, I. Santos, *Q. J. Nucl. Med. Mol. Imaging* **2007**, *51*, 6.
[18] M. S. Balbina, M.Sc. Thesis, University of Lisbon, Lisbon, 2007.
[19] C. F. G. C. Geraldes, A. D. Sherry, W. P. Cacheris, *Inorg. Chem* **1989**, *28*, 3336.
[20] J. Rohovec, M. Kývala, P. Vojtíšek, P. Hermann, I. Lukeš, *Eur. J. Inorg. Chem.* **2000**, 195.
[21] R. Delgado, J. J. R. F. Da Silva, M. T. S. Amorim, M. F. Cabral, S. Chaves, J. Costa, *Anal. Chim. Acta* **1991**, *245*, 271.
[22] F. Kálmán, Ph.D. Thesis, University of Debrecen, Debrecen, 2007.
[23] A. Bianchi, L. Calabi, C. Giorgi, P. Losi, P. Mariani, P. Paoli, P. Rossi, B. Valtancoli, M. Virtuani, *J. Chem. Soc., Dalton Trans.* **2000**, 697.
[24] M. P. C. Campello, S. Lacerda, I. C. Santos, C. F. G. C. Geraldes, J. Vaněk, R. Ševčík, P. Lubal, V. Kubíček, J. Kotek, P. Hermann, E. Tóth, I. Santos, in preparation.
[25] L. Sarka, I. Bányai, E. Brücher, R. Király, J. Platzek, B. Radüchel, H. Schmitt-Willich, *J. Chem. Soc., Dalton Trans.* **2000**, 3699.
[26] R. D. Gillard, P. D. Newman, J. D. Collins, *Polyhedron* **1989**, *8*, 2077.
[27] A. D. Sherry, J. Ren, J. Huskens, E. Brücher, É. Tóth, C. F. C. G. Geraldes, M. M. C. A. Castro, W. P. Cacheris, *Inorg. Chem.* **1996**, *35*, 4604.
[28] F. K. Kálmán, Z. Baranyai, I. Tóth, I. Bányai, R. Király, E. Brücher, S. Aime, X. Sun, A. D. Sherry, Z. Kovács, *Inorg. Chem*. **2008**, *47*, 3851.
[29] P. Táborský, I. Svobodová, Z. Hnatejko, P. Lubal, S. Lis, M. Försterová, P. Hermann, I. Lukeš , J. Havel, *J. Fluoresc.* **2005**, *15*, 507.
[30] É. Tóth, E. Brücher, I. Lázár, I. Tóth, *Inorg. Chem.* **1994**, *33*, 4070.
[31] Z. Piskula, I. Svobodová, P. Lubal, S. Lis, Z. Hnatejko, P. Hermann, *Inorg. Chim. Acta* **2007**, *360*, 3748.
[32] I. Svobodová, Z. Piskula, P. Lubal, S. Lis, P. Hermann, *J. Alloys Compd.* **2008**, *451*, 42.
[33] E. Brücher, G. Laurenczy, Z. S. Makra, *Inorg. Chim. Acta* **1987**, *139*, 141.
[34] A. K. Convington, M. Paabo, R. A. Robison, R. G. Bates, *Anal. Chem.* **1968**, *40*, 700.
[35] C. Frassineti, S. Ghelli, P. Gans, A. Sabatini, M. S. Moruzzi, A. Vacca, *Anal. Biochem.* **1995**, *231*, 374.
[36] M. Maeder, Y.-M. Neuhold, G. Puxty, P. King, *Phys. Chem. Chem. Phys* **2003**, *5*, 2836.

Received May 11, 2009